



HAL
open science

Prediction of ignition delay times of Jet A-1/hydrogen fuel mixture using machine learning

Yunzhe Huang, Chongwen Jiang, Kaidi Wan, Zhenxun Gao, Luc Vervisch, Pascale Domingo, Yong He, Zhihua Wang, Chun-Hian Lee, Qiaoyan Cai, et al.

► **To cite this version:**

Yunzhe Huang, Chongwen Jiang, Kaidi Wan, Zhenxun Gao, Luc Vervisch, et al.. Prediction of ignition delay times of Jet A-1/hydrogen fuel mixture using machine learning. *Aerospace Science and Technology*, 2022, 127, pp.107675. 10.1016/j.ast.2022.107675 . hal-03784193

HAL Id: hal-03784193

<https://normandie-univ.hal.science/hal-03784193>

Submitted on 22 Sep 2022

HAL is a multi-disciplinary open access archive for the deposit and dissemination of scientific research documents, whether they are published or not. The documents may come from teaching and research institutions in France or abroad, or from public or private research centers.

L'archive ouverte pluridisciplinaire **HAL**, est destinée au dépôt et à la diffusion de documents scientifiques de niveau recherche, publiés ou non, émanant des établissements d'enseignement et de recherche français ou étrangers, des laboratoires publics ou privés.

Prediction of Ignition Delay Times of Jet A-1/hydrogen Fuel Mixture Using Machine Learning

Yunzhe Huang^a, Chongwen Jiang^a, Kaidi Wan^{a,*}, Zhenxun Gao^a, Luc Vervisch^b, Pascale Domingo^b, Yong He^c, Zhihua Wang^c, Chun-Hian Lee^a, Qiaoyan Cai^d, Jieping Liu^d

^a*Aircraft and Propulsion Laboratory, Ningbo Institute of Technology & National Laboratory for Computational Fluid Dynamics, School of Aeronautic Science and Engineering, Beihang University, Beijing 100191, China*

^b*CORIA – CNRS, Normandie Université, INSA de Rouen, 76801 Saint-Etienne-du-Rouvray, France*

^c*State Key Laboratory of Clean Energy Utilization, Zhejiang University, Hangzhou 310027, China*

^d*China Academy of Launch Vehicle Technology, Beijing 100076, China*

Abstract

To control the global warming trends, carbon footprint of all the human activities needs to be restricted, including the aviation industry. Mixing hydrogen with commercial kerosene jet fuels appears as a promising alternative fuels to reduce the carbon dioxide emissions of aviation engines. The addition of hydrogen could significantly impact the auto-ignition process of aviation fuels, which is a key ingredient of engine reliability. However, accurate calculations or measurements of ignition delay times over a wide range of pressures, temperatures and fuel blending ratios are complicated and time-consuming. To achieve real-time prediction of ignition delay time for hydrogen-blended jet fuels under various operating conditions, machine learning methods are in-

*Corresponding author.

Email address: wankaidi@buaa.edu.cn (Kaidi Wan)

roduced to build a data-driven proxy model in this work. First, the ignition delay times of Jet A-1/hydrogen fuel mixture are simulated using the well-known HyChem combustion reaction mechanism under different pressures, temperatures, equivalence ratios and blending molar ratios of hydrogen. After some validation against experimental results, an artificial neural network (ANN) model is trained using the database of ignition delay times. Furthermore, a sub-ANN is nested to the original ANN model as an improvement on certain local conditions. The results show that the increase of hydrogen blending ratios can generally accelerate the auto-ignition process except when the temperature is quite low. The ANN models predict the ignition delay times of Jet A-1/hydrogen fuel mixture with good generalization ability and minor computational cost. Moreover, the model prediction accuracy is significantly improved with the nested sub-ANN approach.

Keywords: hydrogen addition, kerosene fuel, ignition delay time, HyChem mechanism, artificial neural network

1. Introduction

With the increasing concern for global warming and pollutant emissions from aviation transportation, researchers are focusing on finding alternative fuels with high thermal efficiency and clean emission characteristics [? ?]. Hydrogen is considered as one of the most promising clean fuels because of its high energy density per mass and zero carbon-related emissions [?]. Airbus has released “ZEROe” project which aims to develop the world’s first zero-emission commercial aircraft by 2035. Liquid hydrogen is used as fuel for modified gas turbine engines to power the “ZEROe” concept aircraft [1].

10 However, the production capacity of hydrogen still needs to be developed
11 to fully replace conventional fossil fuels [2]. In this context, one practical
12 approach to progressively improve the combustion and emission character-
13 istics of aircraft engines is to combine hydrogen with fossil fuels [3–6]. Jet
14 A-1 is a type of conventional aviation fuel widely used in aircraft engines,
15 which therefore plays an important role in aviation transportation industry
16 [7, 8]. With the help of hydrogen addition, the concern for carbon dioxide
17 and pollutant emissions of burning Jet A-1 fuel could be mitigated.

18 Although the Jet A-1/hydrogen fuel mixture has many advantages in the
19 aspect of emission, the design of engine needs to be reassessed since the
20 fuel combustion characteristics change due to the addition of hydrogen. As
21 one of the key issues, ignition and flame stabilization must be maintained
22 with this novel fuel. The complex ignition processes under various engine
23 operating conditions can be quantified by the ignition delay time (IDT), an
24 important parameter for engine design [9]. IDT can be determined from
25 measurements in rapid compression machine and shock tube experiments
26 [10? , 11], so that the modeling of chemistry can be calibrated for numerical
27 simulations [12?]. In the present study, zero-dimensional (0-D) auto-ignition
28 processes of Jet A-1/hydrogen fuel mixture with air are simulated to collect
29 the IDTs. The state-of-the-art HyChem (Hybrid Chemistry) model [13, 14]
30 is introduced, which shows a good efficiency and accuracy in predicting the
31 global combustion properties of jet fuels [13]. The combustion chemistry of
32 Jet A-1 fuel is first modeled by lumped reaction steps for pyrolysis supported
33 by experimental data, and then detailed reaction mechanism is applied to the
34 oxidation process of the pyrolysis products.

35 Recently, machine learning (ML) methods like artificial neural network
36 (ANN) have been introduced to research combustion [15], flame [?], and
37 ignition process [16]. ANN shows great potential of non-linear regression in
38 tabulating and order reduction, which leads to better prediction with less
39 memory and CPU-time cost [15, 17, 18], also to analyze experimental mea-
40 surements [19]. Since accurate numerical simulation of 0-D auto-ignition pro-
41 cesses using detailed chemical reaction mechanisms is a quite time-consuming
42 process due to solving many degrees of freedom, it is practically useful to de-
43 velop an quasi-instant ANN proxy model (or digital-twin) for predicting IDTs
44 over a wide range of temperatures, pressures and other parameters relevant
45 to guide engine designs. Such ANN proxy models have been developed in
46 previous studies for hydrogen [20], biodiesel [21] and n-heptane [22]. In ad-
47 dition, recent studies pay more attention to the ML modeling of IDTs of
48 complex mixture fuels. For instance, ML-based IDT models have been de-
49 veloped by Han et al. [9] for methane-dimethyl ether dual fuel, by Jach et
50 al. [23] for various C1C7 hydrocarbonO₂Ar mixtures, and by Cui et al. [24]
51 for n-butane/hydrogen mixtures. However, it is quite challenging to built a
52 single ML/ANN model to accurately predict IDTs of complex mixture fuels
53 under a wide range of engine operating conditions.

54 To improve the performance of ANN model on complex problems with
55 a high-dimensional distribution of database, new approaches have been in-
56 troduced into the ANN framework, e.g., clustering [25], multiple multilayer
57 perceptrons [26] and many others [27–29]. To address the large scale of
58 database, Nguyen et al. [25] divide and cluster the entire database to assem-
59 ble sub-datasets with similar characteristics. Ding et al. [26] employ multiple

60 multilayer perceptrons to balance relative errors in small and large compo-
61 sition changes. The non-uniform data distribution in a large scale database
62 can results in the problem of poor local prediction of ANN model, which
63 deserves special attentions during the implementation of ANN framework.

64 The first aim of the present study is to explore the feasibility of using
65 a data-driven ANN proxy model to predict IDTs of Jet A-1/hydrogen fuel
66 mixture under various engine representative operating conditions. The Hy-
67 Chem A1NTC reaction mechanism [13] is employed with 0-D auto-ignition
68 simulations to build the IDTs database covering different pressures, temper-
69 atures, equivalence ratios and blending molar ratios of hydrogen, which is
70 required for training the ANN model. The second aim is to investigate the
71 performance of nested sub-ANN approach, in which a sub-ANN model is
72 nested to the original basic ANN model as an improvement on certain local
73 conditions.

74 The rest of this paper is structured as follows. Section 2 explains the 0-
75 D auto-ignition simulation method, IDT database construction, basic ANN
76 model, and nested sub-ANN approach. In Section 3, results of the 0-D auto-
77 ignition simulation and ANN model are compared and discussed. Specifically,
78 further validation of HyChem mechanism against experimental data and the
79 analyses of IDTs for Jet A-1/hydrogen fuel mixture are presented in Section
80 3.1. Then the performance of the basic ANN model is discussed in Section 3.2
81 while the improvement of the nested sub-ANN approach is shown in Section
82 3.3. Finally, the main conclusions of the present study are summarized in
83 Section 4.

84 **2. Methodology**

85 *2.1. Numerical method*

86 0-D simulations for the auto-ignition process of Jet A-1/hydrogen fuel
87 mixture with air are performed using the HyChem mechanism [13]. Ignition
88 delay processes are simulated in a constant volume and adiabatic reactor at
89 specified initial temperatures and pressures to investigate ignition delay time.
90 The open source library of python for chemical kinetics Cantera 2.4.0 [30] is
91 used to simulate the ignition process with the HyChem mechanism.

92 Since the HyChem mechanism is originally developed for the Jet A-1
93 fuel, it is necessary to justify its application to the Jet A-1/hydrogen fuel
94 mixture. However, the experimental IDT results of Jet A-1/hydrogen fuel
95 mixture are unavailable yet. Hence, the auto-ignition processes of Jet A-1
96 and hydrogen are simulated using the HyChem mechanism and compared
97 against experimental IDT results of Jet A-1 and hydrogen, respectively. The
98 validation results will be shown in Section 3.1. After this validation, the
99 HyChem mechanism is considered as applicable to the Jet A-1/hydrogen
100 fuel mixture.

101 *2.2. Database construction*

102 To develop a data-driven proxy model for predicting IDT of Jet A-1/hydrogen
103 fuel mixture, a database constitute of adequate training data is required.
104 Here, the database is four dimensional which involves temperatures (T),
105 pressures (P), equivalence ratios (ϕ) and blending molar ratios of hydro-
106 gen (R) as the feature channels. As summarized in Table 1, the IDTs of
107 Jet A-1/hydrogen fuel mixture are simulated taking different combinations

108 of the four features in the range of $P = 1.0 \sim 20.0$ atm, $T = 800 \sim 1600$ K,
 109 $\phi = 0.5 \sim 1.5$, and $R = 0 \sim 0.5$ as the initial conditions.

110 Finally, the entire database contains 104,000 samples of IDT determined
 111 from 0-D auto-ignition simulations. Figure 1 shows the non-uniform distri-
 112 bution of the obtained IDTs spanning multiple scales from $1 \mu\text{s}$ to $10^5 \mu\text{s}$. It
 113 features a typical long tail distribution. IDTs with extremely low values are
 114 the vast majority (75% of IDTs are below $1692 \mu\text{s}$) while a few IDTs take
 115 quite high values. In this case, the data-driven proxy model can be more
 116 difficult to train or have lower accuracy because of the outliers with high
 117 values.

Table 1: Initial conditions of 0-D auto-ignition simulations to generate IDT database of Jet A-1/hydrogen fuel mixture.

Feature	Range	Division Value
Pressure (atm)	$1.0 \sim 20.0$	1.0
Temperature (K)	$800 \sim 1600$	10
Equivalence ratio (-)	$0.5 \sim 1.5$	0.1
Blending molar ratio of hydrogen (-)	$0 \sim 0.5$	0.1

118 2.3. Artificial neural network model

119 To perform highly nonlinear regression of the IDT database, a single ANN
 120 model is first introduced as the basic data-driven proxy model for predicting
 121 IDTs of Jet A-1/hydrogen fuel mixture. The ANN model has multiple hidden
 122 layers with fully connected neurons in each layer. As shown in Fig. 2, the
 123 basic ANN has an input layer with 4 neurons corresponding to the four input
 124 features, i.e., the z-score normalized pressure, temperature, equivalence ratio

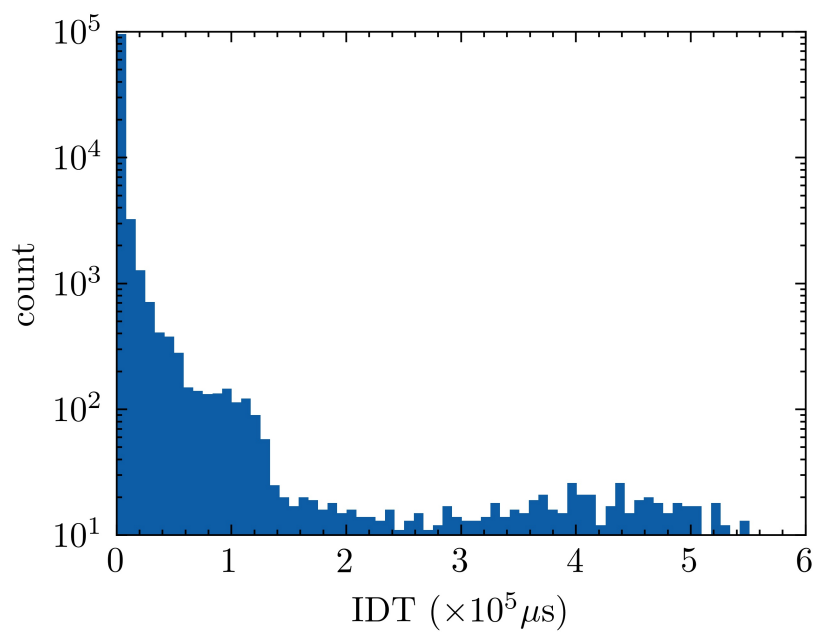


Figure 1: Long tail distribution of IDT (ignition delay time) values of Jet A-1/hydrogen fuel mixture in the obtained database containing 104,000 samples.

125 and blending molar ratio of hydrogen. 5 hidden layers are employed with
 126 80 neurons in each layer. Rectified linear unit (ReLU) function is set as the
 127 activation function of every neuron. The label of the output layer is the
 128 logarithmic normalized IDT, which is expressed as

$$y' = \frac{\ln(y)}{\ln(y_{\max})}, \quad (1)$$

129 where y represents the IDT and y' is the normalized IDT. Table 2 summarizes
 130 the details of the basic ANN model, which contains in total 26,401 trainable
 131 parameters of weights and biases. The model is built with TensorFlow 2.4.1
 132 [31], an open-source machine learning framework in Python.

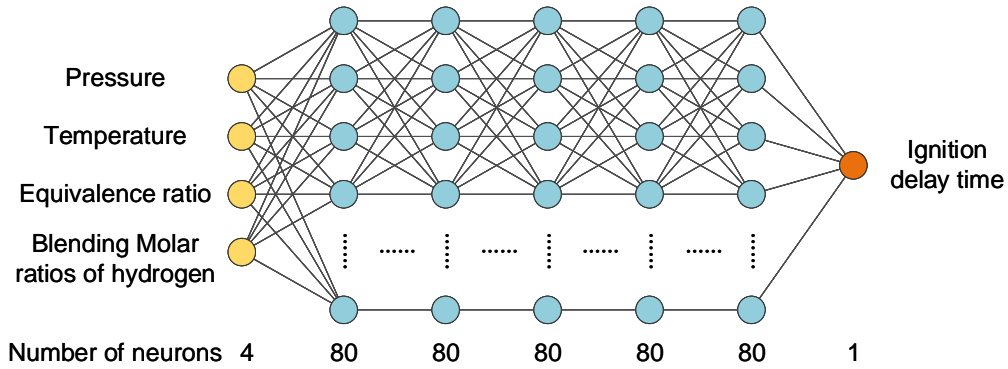


Figure 2: Structure of the basic ANN model. 4 input features: pressure, temperature, equivalence ratio and blending molar ratio of hydrogen. 5 hidden layers with 80 neurons in each one. Output layer: IDT.

133 The entire IDT database is divided into training set and testing set, with
 134 the proportion of 80% and 20%, respectively. The model is trained by the
 135 Adam optimization algorithm [32] to minimize the loss function of Mean
 136 Square Error (MSE) in Eq. (2).

$$\text{MSE} = \frac{1}{n} \sum_{i=0}^n (y_i - \hat{y}_i)^2, \quad (2)$$

137 where n is the number of samples, while y_i and \hat{y}_i are the true value and
 138 prediction of the i -th sample, respectively. In the training procedure, the
 139 whole training database is decomposed to 2080 batches with 40 data points
 140 per batch to train the ANN for 500 epoches. The learning rate is initially set
 141 to 10^{-3} and gets reduced by 20% each time if the MSE loss does not drop
 142 for 10 epochs during the training. The lower limit of the learning learning
 143 rate is set to 10^{-5} . To better evaluate the prediction performance of the
 144 ANN, Mean Relative Error (MRE) in Eq. (3) is calculated as an additional
 145 indicator.

$$\text{MRE}(\%) = \frac{100}{n} \sum_{i=0}^n \left| \frac{y_i - \hat{y}_i}{y_i} \right|. \quad (3)$$

146 2.4. Nested sub-ANN approach

147 In this section, we propose a nested sub-ANN approach to further improve
 148 the prediction performance over the wide IDT range from $1 \mu\text{s}$ to $10^5 \mu\text{s}$.
 149 Because of the long tail distribution of the IDT database (Fig. 1), numerous
 150 data points with low IDT and few ones with high IDT appear in the database
 151 together, leading to adverse effects on the training of the ANN model. For
 152 instance, the outliers with high IDT have a larger impact on the loss function
 153 of Eq. 3 than the data points with low IDT. The optimization of the ANN
 154 prediction on these low IDT data points then becomes difficult since their
 155 contributions on the loss function are minor. To improve this situation, a
 156 sub-ANN is trained specially for the conditions where the basic ANN make
 157 poor predictions.

Table 2: Structures of the basic ANN and nested sub-ANN models

Model	Total parameters	Layer type	Neuron number	Activation function
ANN	26,401	Input	4	—
		Dense	80	ReLU
		Dense	80	ReLU
		Dense	80	ReLU
		Dense	80	ReLU
		Dense	80	ReLU
		Dense(Output)	1	—
sub-ANN	10,801	Input	4	—
		Dense	64	ReLU
		Dense	64	ReLU
		Dense	48	ReLU
		Dense	64	ReLU
		Dense	64	ReLU
		Dense(Output)	1	—

158 The data points with $IDT < 10^3 \mu s$ are collected from the original
159 database to train the sub-ANN model. As summarized in Table 2, the sub-
160 ANN model has a lighter structure than the basic ANN, because the subset
161 contains fewer and more concentrated data points. By reducing the number
162 of hidden layers to 4 and cutting down neuron numbers, the sub-ANN model
163 has only 10,801 trainable parameters.

164 The overall training and predicting processes of the nested sub-ANN ap-
165 proach is demonstrated in Fig. 3. For the training process, the data points
166 with $IDT < 10^3 \mu s$ featuring a large local relative error during the basic ANN
167 training are collected to form a subset database. A sub-ANN is then trained
168 only with the subset and nested to the basic ANN, appearing as a combined
169 dual-ANN model. For the predicting process, the IDT is first predicted by

170 the basic ANN with the input features. Then, if the predicted IDT falls in
171 the governing region of the sub-ANN, i.e., $< 10^3 \mu\text{s}$, it is predicted again by
172 the sub-ANN to be the final prediction.

173 3. Results and discussion

174 3.1. Ignition delay time

175 Figure 4 shows the comparison between the simulated IDTs using the
176 HyChem mechanism and experimental data [33, 34] of Jet A-1 in the range
177 of $P = 3 \sim 15 \text{ atm}$, $T = 650 \sim 1400 \text{ K}$ and $\phi = 0.5 \sim 1.5$. In Fig. 4(a),
178 the simulated IDTs agree well with the experimental data [33] in the linear
179 region at the pressure of 3, 6 and 12 atm compared. Figure 4(b) shows
180 that the negative temperature coefficient (NTC) characteristic of the Jet A-
181 1 can be generally well captured by the HyChem mechanism, although the
182 simulated NTC regions appear at higher temperatures with lower IDTs in
183 comparison to the experimental data [34]. Overall, the simulation profiles of
184 IDT versus temperature of the Jet A-1 by the HyChem mechanism have a
185 good agreement with the experimental measurements.

186 Figure 5 shows the profiles of IDT versus temperature of hydrogen at
187 4.0/16.0 atm under fuel-lean, stoichiometric and fuel-rich conditions. The
188 simulated IDTs of hydrogen by the HyChem mechanism match well with the
189 experimental measured IDTs [35] under those various conditions. Compared
190 to the Jet A-1 fuel, hydrogen does not show the NTC characteristic and its
191 IDT increase monotonically with the temperature decreasing.

192 The above results demonstrate that the HyChem mechanism can capture
193 the auto-ignition process of Jet A-1 and hydrogen fuels reasonably well. On

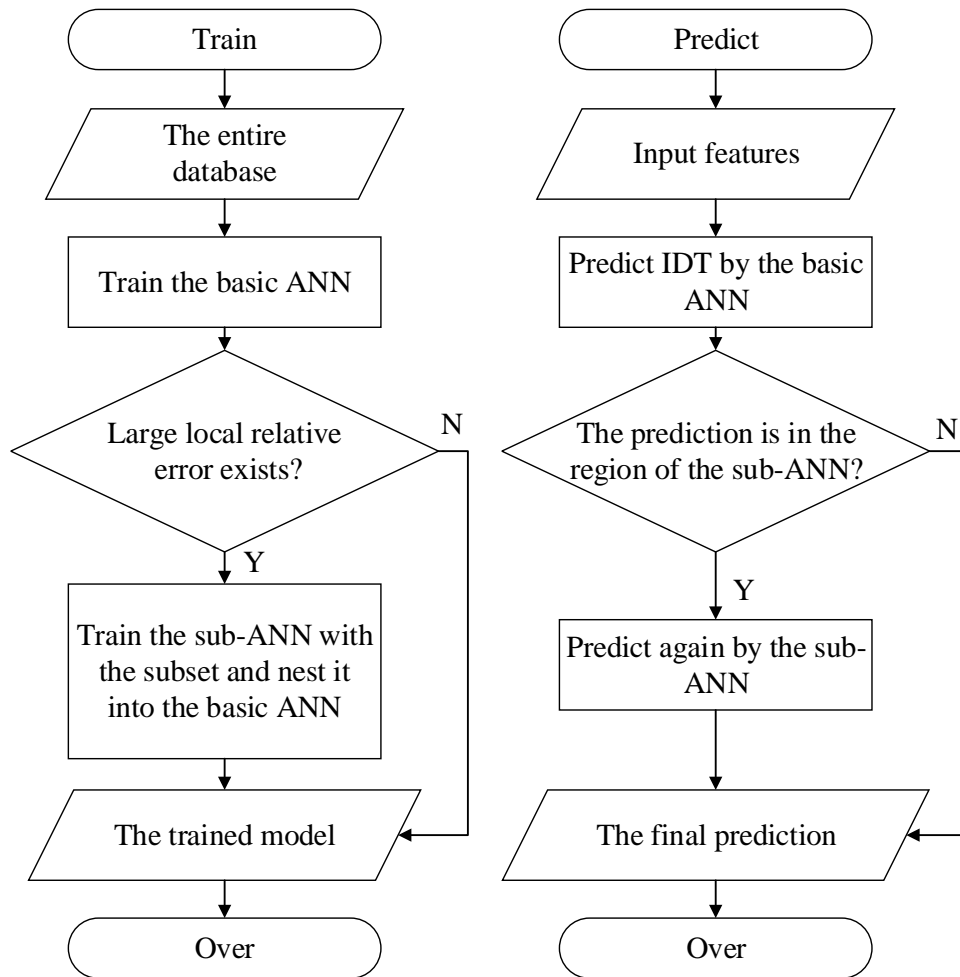
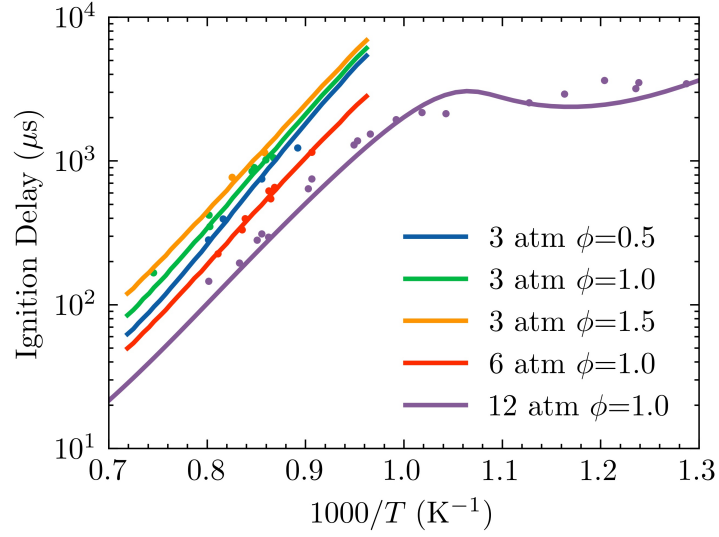
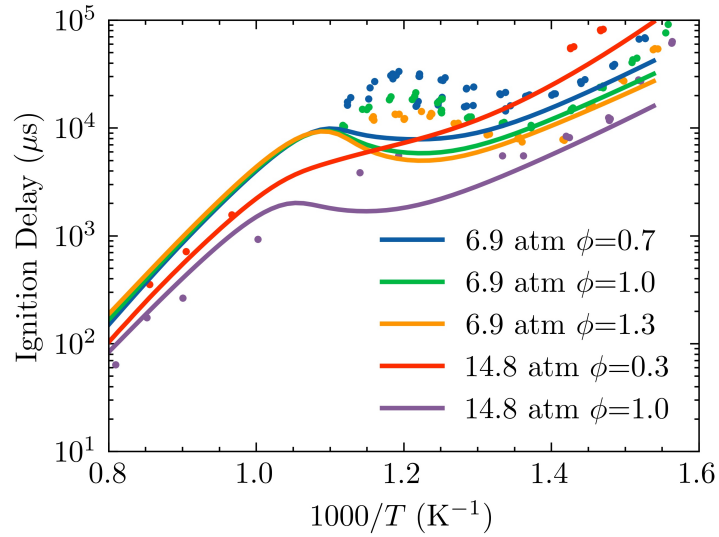


Figure 3: Flowchart of the overall training (left) and predicting (right) processes of the nested sub-ANN approach.



(a)



(b)

Figure 4: Comparisons between the HyChem simulated (lines) and experimental measured (symbols) IDTs of Jet A-1 under various temperature, pressure and equivalence ratio conditions.

194 that basis, the HyChem mechanism is regarded as applicable for the auto-
 195 ignition simulations of Jet A-1/hydrogen fuel mixture. The IDT database
 196 of the Jet A-1/hydrogen fuel mixture is then built by varying the initial
 197 conditions, i.e., temperature, pressure, equivalence ratio and blending molar
 198 ratio of hydrogen. Part of the IDT database is shown in Figs. 6 and 8.

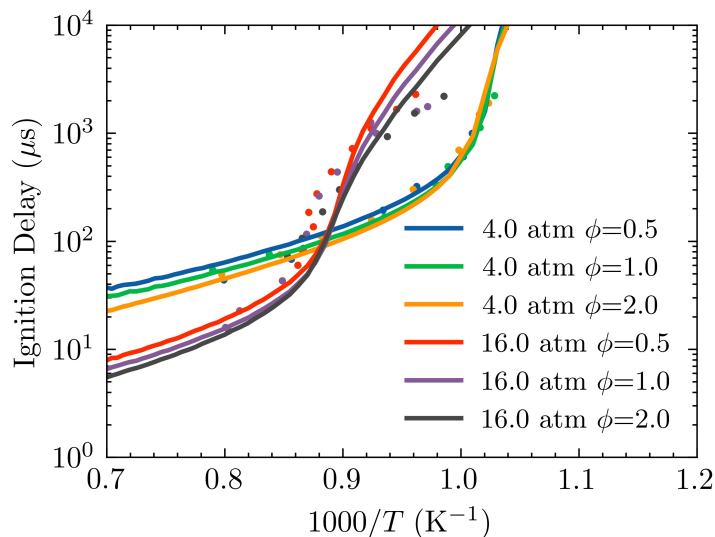


Figure 5: Comparisons between the HyChem simulated (lines) and experimental measured (symbols) IDTs of hydrogen under various temperature, pressure and equivalence ratio conditions.

199 Figure 6 shows the characteristics of IDT of the mixture fuel with various
 200 blending molar ratio of hydrogen addition in the temperature range of $T =$
 201 $800 \sim 1600$ K, at $p = 1, 5, 10$ and 20 atm and $\phi = 1.0$. In the range of
 202 $T > 1000$ K, the logarithmic IDT keeps an almost linear relationship with
 203 T^{-1} , while the hydrogen addition have only slight influence on the IDT.
 204 Specifically, the IDT gets shorter with the increase of blending molar ratio of
 205 hydrogen. Besides, the influence becomes more apparent at relatively lower

206 temperatures in this linear region, e.g., at the peak of IDTs plotted in Fig.
207 6(b). Notably, the opposite trend can appear at the NTC region where the
208 hydrogen addition leads to a longer IDT at low temperatures. For example in
209 Fig. 6(c), the reverse of the hydrogen addition effects on IDT occurs around
210 $T < 820$ K under the pressure $P = 10$ atm.

211 The opposite effects of hydrogen addition depending on temperature has
212 also been reported in previous studies on hydrogen blending with methyl
213 butanoate [36] and n-heptane/n-decane [37]. The OH radical-related reaction
214 rates decrease at low temperatures but increase at high temperatures upon
215 hydrogen addition, leading to the change of production rates of the OH,
216 HO₂ and H₂O₂ radicals [36]. Figure 7 shows that the OH mass fraction gets
217 lower at 800 K but higher at 900 K with the increasing blending ratio of
218 hydrogen. Hence, hydrogen acts as an ignition inhibitor of the fuel mixture
219 at low temperatures such as 800 K, but it promotes the ignition process at
220 higher temperature, e.g., 900 K.

221 In Fig. 8, the changes of IDT of Jet A-1/hydrogen fuel mixture over
222 pressures are shown by the curves colored by pressure from 1 atm to 20
223 atm. The blending molar ratio of hydrogen is fixed as 50%. The bright zones
224 featuring a high pressure get lower IDT compared to the dark zones featuring
225 a low pressure, which means increasing pressure can reduce IDT for the
226 hydrogen-enriched mixture fuel. On the other hand, the NTC characteristic
227 of the Jet A-1/hydrogen fuel mixture becomes less obvious as the pressure
228 increase. Especially for $P = 20$ atm, the NTC characteristic gets disappear
229 and the IDT increase monotonically as the temperature decreases.

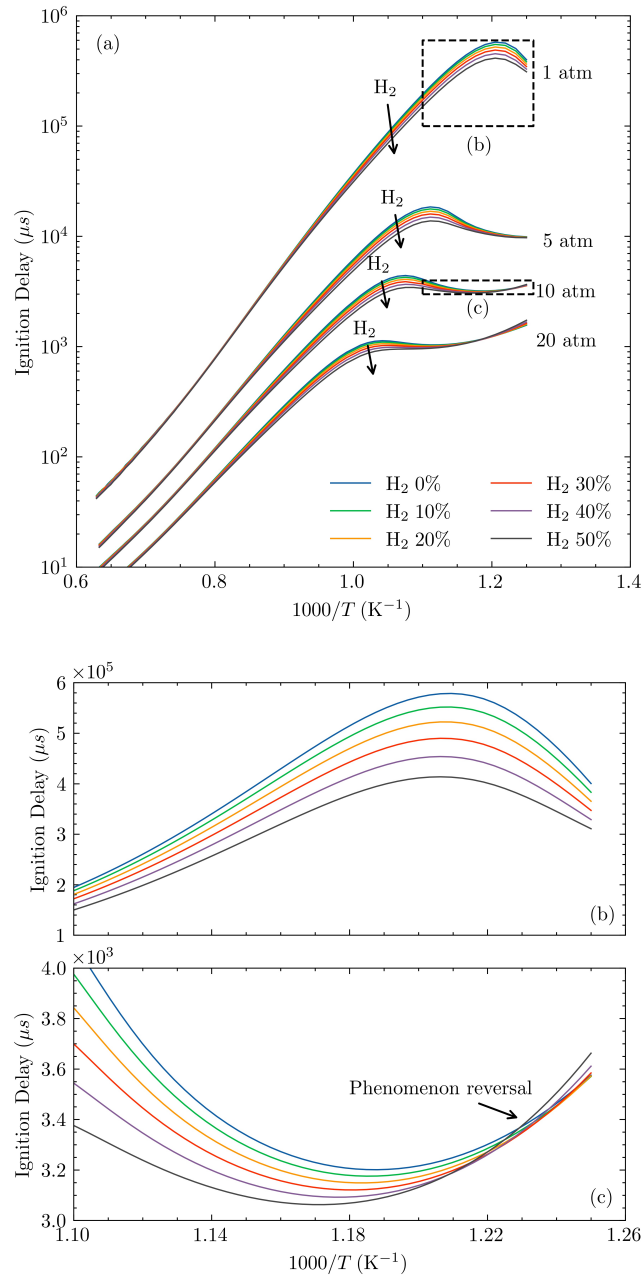
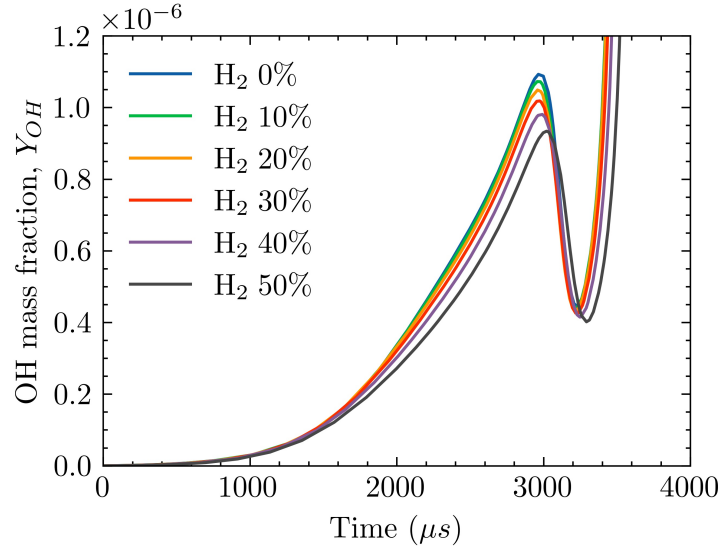
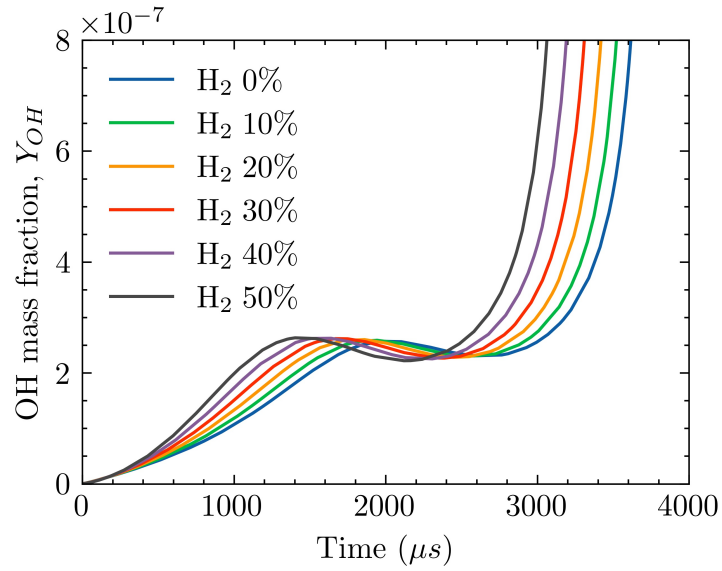


Figure 6: HyChem simulated IDTs of Jet A-1/hydrogen fuel mixture at $\phi = 1.0$. (a) The blending molar ratio of hydrogen increases in the arrow direction for each pressure group profiles; (b) Zoomed-in profiles for $P = 1$ atm; (c) Zoomed-in profiles for $P = 10$ atm.



(a) 800 K



(b) 900 K

Figure 7: Time evolution of OH mass fraction during the ignition process of Jet A-1/hydrogen fuel mixture at $P = 10$ atm and $\phi = 1.0$.

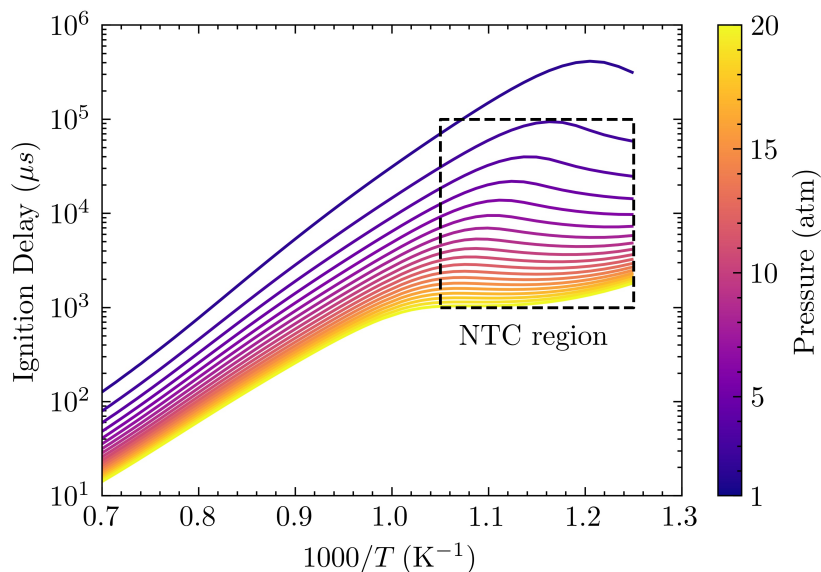


Figure 8: HyChem simulated IDTs of Jet A-1/hydrogen fuel mixture at $\phi = 1.0$ and $R = 50\%$. The pressure between 1 atm and 20 atm is indicated by the color of the curves.

230 *3.2. Prediction of the basic ANN model*

231 The comparisons between the predicted IDTs by the basic ANN model
 232 and the simulated IDTs using the HyChem mechanism, which are seen as
 233 the reference true values, are shown in Figs. 9 and 10.

234 Performance of the trained basic ANN model is evaluated on the test set
 235 containing 20,800 data points. Figure 9 shows the good agreement between
 236 ANN predictions and reference true values and the correlation coefficient
 237 R^2 reaches 0.9994. The MRE of the ANN predictions is 1.0377%, and the
 238 relative error mainly locates in the range of $\pm 5\%$ with a normal distribution.

239 The comparison between the simulated IDT profiles by the HyChem
 240 mechanism and predictions by the basic ANN model are shown in Fig. 10,
 241 in which four typical cases are plotted as examples. The predictions by the

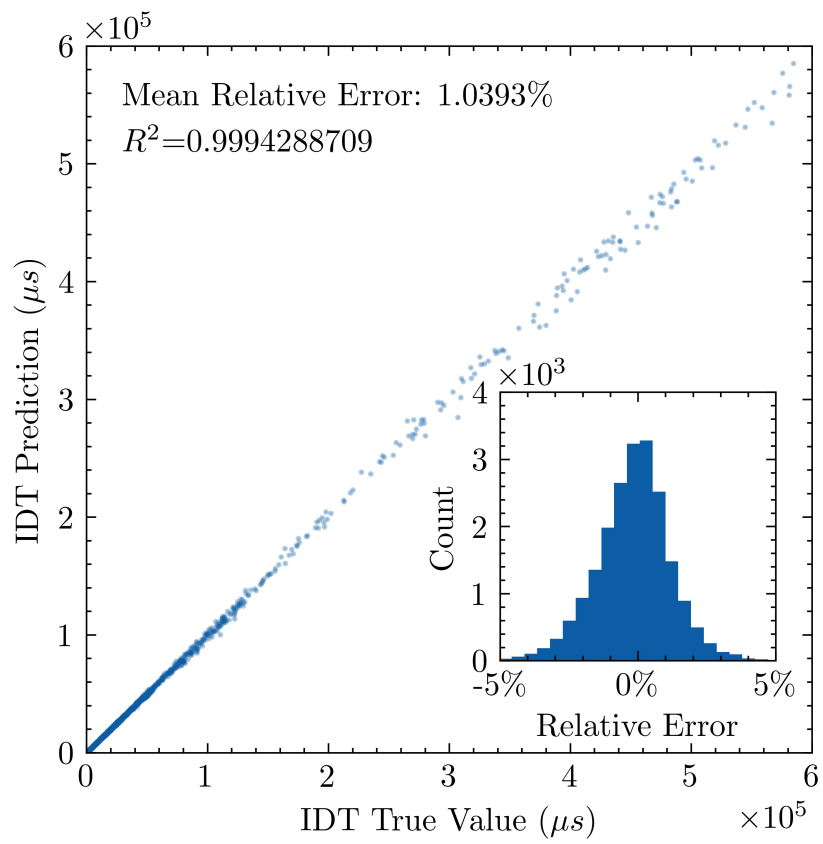


Figure 9: Comparison between the IDT reference true values and the predictions by the basic ANN on the test set. The subplot shows the distribution of relative errors.

242 ANN model are in good agreement with the HyChem simulation results.
 243 Though, the subplot shows a slight departure in Case I under high temper-
 244 ature conditions.

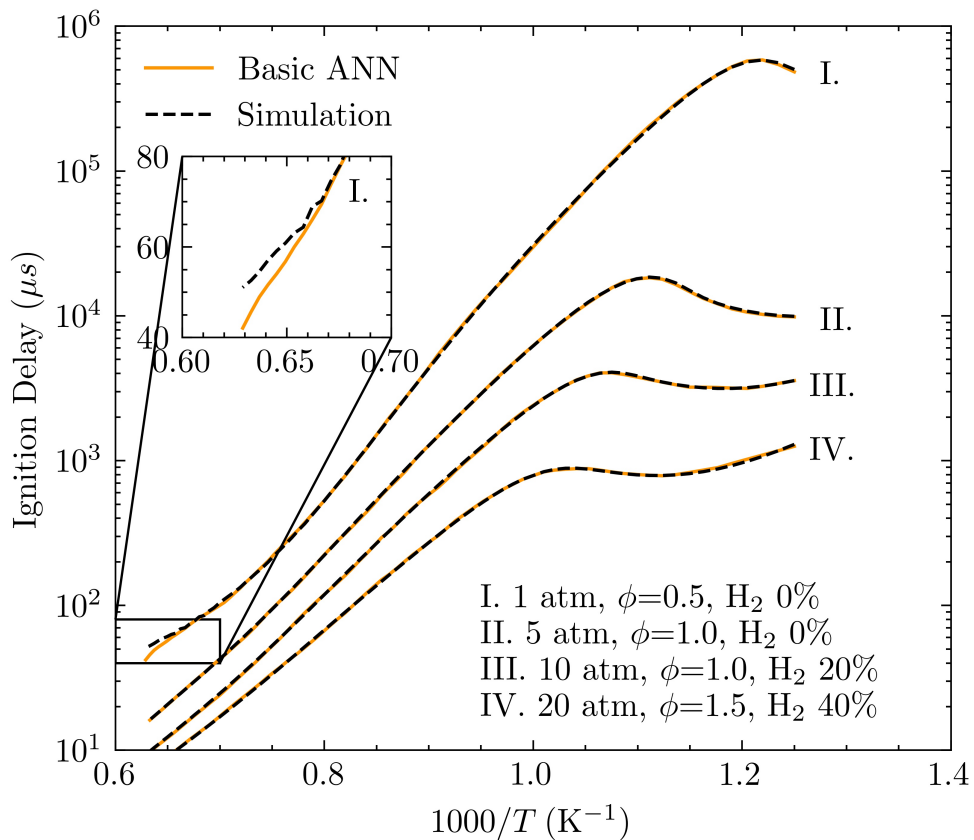


Figure 10: Comparison between the HyChem simulated IDT profiles and the basic ANN predictions under various pressure, equivalence ratio and hydrogen blending ratio conditions. The subplot is the zoomed-in view of the Case I.

245 *3.3. Improvement with the nested sub-ANN model*

246 In order to control the departures observed under high temperature con-
 247 ditions, as proposed above a sub-ANN is nested to the basic ANN to improve

248 the IDT predictions.

249 Figure 11(a) illustrates the distribution of relative errors of the basic ANN
250 prediction. The subplot shows that some outliers with extremely low IDT
251 can have large relative errors up to 10%. Besides, the probability density
252 curves have flat circular shapes, indicating data points with low IDTs are
253 more likely to have larger relative errors.

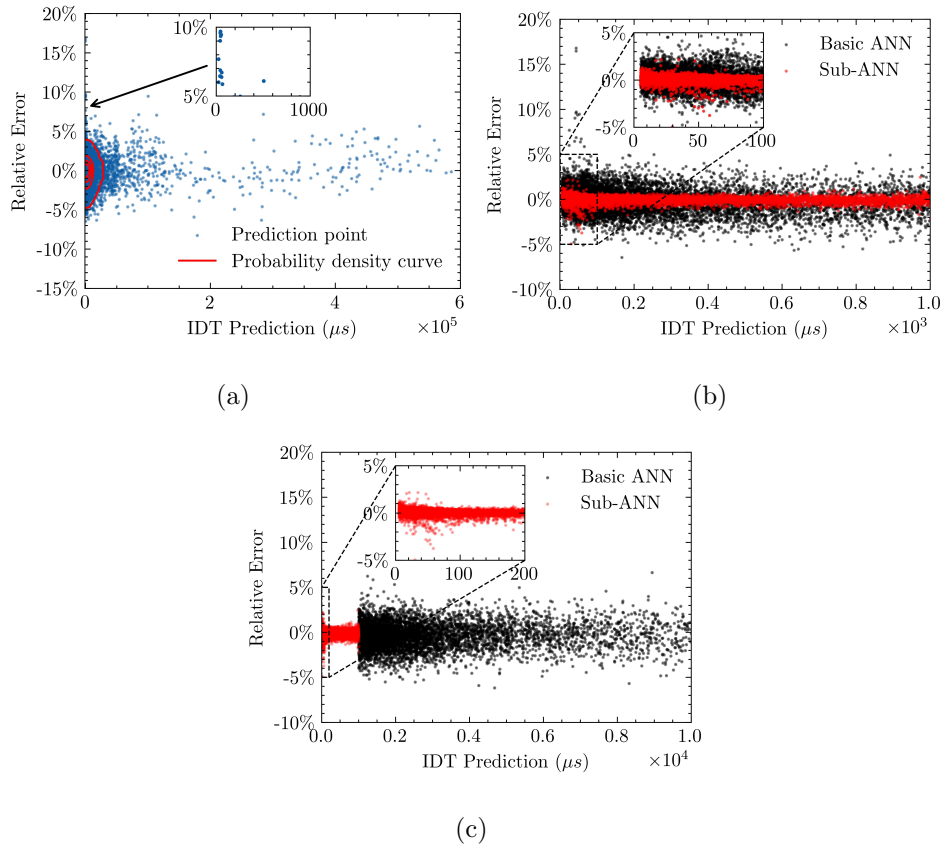


Figure 11: Scatter plots of relative errors against IDT predictions by the ANN models. (a) Results of the basic ANN model. (b) Comparison between the basic ANN and the sub-ANN for IDT < $10^3 \mu s$. (c) Results of the combined dual-ANN model.

254 The relative errors of the basic ANN (black dots) and the sub-ANN (red

255 dots) for the subset data with $\text{IDT} < 10^3 \mu\text{s}$ are compared in Fig. 11(b).
256 The relative error of the sub-ANN is obviously lower than the basic ANN,
257 although the subplot shows the performance of the sub-ANN deteriorates
258 in the range of $\text{IDT} < 100 \mu\text{s}$. If a higher accuracy is required, another
259 nested sub-ANN can be introduced to deal with the smaller range of data.
260 Figure 11(c) shows the relative error distributions of the combined dual-ANN
261 model. It can be observed that the prediction accuracy for the low IDT region
262 has been significantly improved with the nested sub-ANN approach, as the
263 relative error is reduced to $\pm 5\%$.

264 Figure 12 compares the IDT profiles of 9 typical cases in the high tem-
265 perature region among the HyChem simulations, basic ANN predictions and
266 predictions by the nested sub-ANN approach. The blue dashed lines, rep-
267 resenting the nested sub-ANN predictions, exactly overlap the black lines
268 representing the HyChem simulation results. Hence, the nested sub-ANN
269 approach is an effective method to improve ANN accuracy by reducing large
270 local relative errors.

271 Table 3 compares the normalized CPU time cost among the HyChem
272 simulation, the basic ANN and the nested sub-ANN approaches for predicting
273 IDTs of the 9 cases in Fig. 12. The basic ANN model is 10^3 times faster
274 than the HyChem simulation method. The nested sub-ANN model is slower
275 than the basic one because two ANNs are used to improve the prediction
276 accuracy. However, since its CPU cost is still much lower than the HyChem
277 simulation, the nested sub-ANN approach is worth to employ.

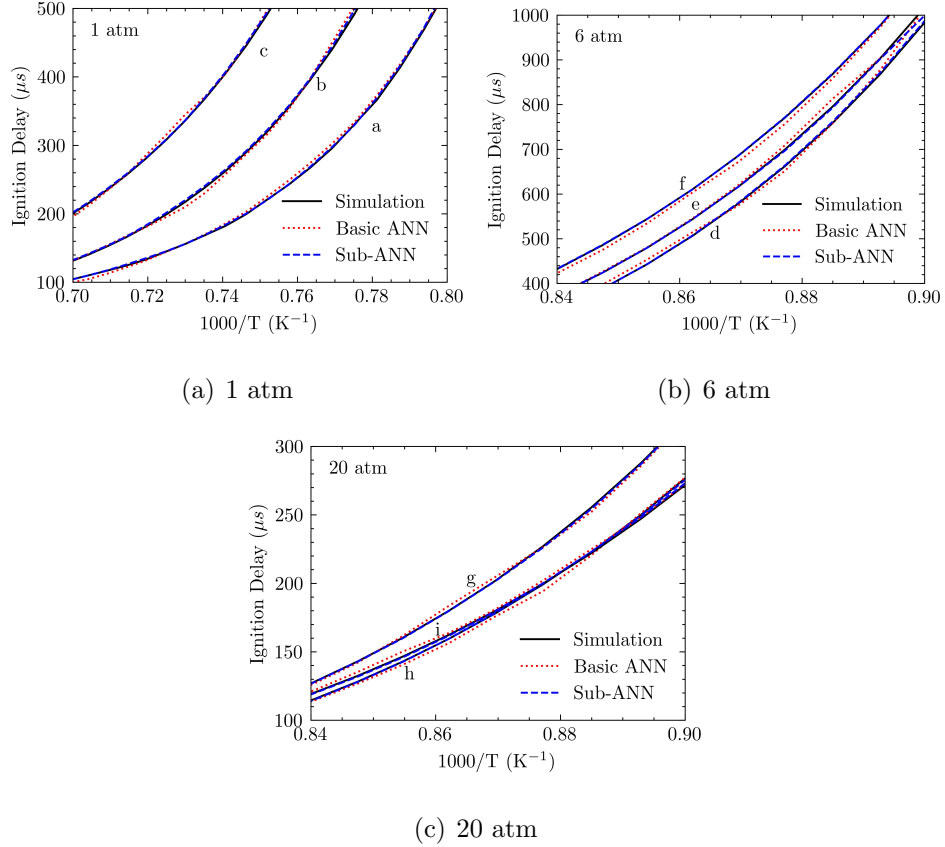


Figure 12: Comparison of the IDT profiles predicted by HyChem simulation, the basic ANN and the nested sub-ANN approach. 9 typical cases are plotted. Case a: $\phi = 0.5, R = 0\%$. Case b: $\phi = 1.0, R = 20\%$. Case c: $\phi = 1.5, R = 40\%$. Case d: $\phi = 0.5, R = 0\%$. Case e: $\phi = 1.0, R = 20\%$. Case f: $\phi = 1.5, R = 40\%$. Case g: $\phi = 0.5, R = 0\%$. Case h: $\phi = 1.0, R = 20\%$. Case i: $\phi = 1.5, R = 40\%$.

Table 3: Normalized Averaged CPU time cost of HyChem simulation and ANN proxy models to predict IDTs. (Normalization by the basic ANN model)

HyChem	Basic ANN	Nested sub-ANN
1493.7	1.0	2.0

278 4. Conclusions

279 In this work, the ignition delay times (IDTs) of Jet A-1/hydrogen fuel
280 mixture under a wide range of operating conditions, including various tem-
281 peratures, pressures, equivalence ratios and blending molar ratios of hydro-
282 gen, are numerically investigated first. Zero-dimensional auto-ignition simu-
283 lations of the fuel mixture with air are performed using the HyChem mecha-
284 nism [13] to obtain the IDTs. The IDT vs. T^{-1} profiles of Jet A-1/hydrogen
285 fuel mixture feature both a linear region and a negative temperature coeffi-
286 cient (NTC) region. The addition of hydrogen can shorten the IDTs of the
287 mixture in most cases especially under high temperatures, while this effect
288 is not obvious under the conditions with both a low temperature and a high
289 pressure. Moreover, hydrogen is found to increase the IDTs of the mixture
290 at temperature lower than 820 K. It means hydrogen can act as ignition pro-
291 moter or inhibitor of the fuel mixture under different operating conditions.

292 With the help of numerical simulation, an IDT database of Jet A-1/hydrogen
293 fuel mixture containing 104,000 data points is built. The performance of
294 data-driven artificial neural network (ANN) modeling approach on predict-
295 ing the IDTs of the mixture fuel is then investigated. A basic ANN model
296 with 5 hidden layers is found to achieve good predictions on the IDTs with
297 a mean relative error of 1%. However, the maximum local relative error can
298 reach up to 10% for the conditions with short IDT. A nested sub-ANN ap-
299 proach is therefore proposed to improve the accuracy of predictions under
300 those conditions with a specialized sub-ANN model nested to the original
301 basic ANN model. The proposed nested sub-ANN approach successfully re-
302 duces the maximum local relative error of ANN predictions to below 5%.

303 The proposed data-driven ANN approaches are around 10^3 times faster than
304 the classic HyChem simulation method on IDT prediction.

305 It should be noted that the developed data-driven ANN models of IDTs
306 of the Jet A-1/hydrogen fuel mixture are trained from purely numerical pre-
307 dictions of the HyChem mechanism, since the experimental IDT results of
308 the Jet A-1/hydrogen fuel mixture are not available yet. However, once the
309 experimental IDT results of the mixture become available in the future, the
310 numerical IDT database can then be calibrated and the proposed data-driven
311 modeling approach can be readily applied.

312 **Acknowledgments**

313 This work was jointly supported by the National Natural Science Foun-
314 dation of China (52076008, 11972061, 11872094, 11721202), the Zhejiang
315 Provincial Natural Science Foundation (LGJ21E060001), and the State Key
316 Laboratory of Clean Energy Utilization (Open Fund Project No. ZJUCEU2020008).

317 **References**

- 318 [1] Airbus, Hydrogen: An important pathway to our zero-emission ambi-
319 tion (2021).
320 URL [https://www.airbus.com/innovation/zero-emission/
321 hydrogen.html](https://www.airbus.com/innovation/zero-emission/hydrogen.html)
- 322 [2] S. Rondinelli, R. Sabatini, A. Gardi, Challenges and Benefits offered by
323 Liquid Hydrogen Fuels in Commercial Aviation, Practical Responses to
324 Climate Change (PRCC), Melbourne, Australia, 2014.

- 325 [3] H. Pan, S. Pournazeri, M. Princevac, J. W. Miller, S. Mahalingam, M. Y.
326 Khan, V. Jayaram, W. A. Welch, Effect of hydrogen addition on criteria
327 and greenhouse gas emissions for a marine diesel engine, *International*
328 *Journal of Hydrogen Energy* 39 (21) (2014) 11336–11345.
- 329 [4] Y. Zhang, Numerical study on auto-ignition characteristics of hydrogen-
330 enriched methane under engine-relevant conditions, *Energy Conversion*
331 *and Management* 200 (2019) 112092.
- 332 [5] S. Lee, S. Song, A rapid compression machine study of hydrogen effects
333 on the ignition delay times of n-butane at low-to-intermediate temper-
334 atures, *Fuel* 266 (2020) 116895.
- 335 [6] J. Chen, X. Jiang, X. Qin, Z. Huang, Effect of hydrogen blending on the
336 high temperature auto-ignition of ammonia at elevated pressure, *Fuel*
337 287 (2021) 119563.
- 338 [7] H. S. Han, C. H. Sohn, J. Han, B. Jeong, Measurement of combus-
339 tion properties and ignition delay time of high performance alternative
340 aviation fuels, *Fuel* 303 (2021) 121243.
- 341 [8] P. Vozka, G. Kilaz, A review of aviation turbine fuel chemical
342 composition-property relations, *Fuel* 268 (2020) 117391.
- 343 [9] W. Han, Z. Sun, A. Scholtissek, C. Hasse, Machine Learning of ignition
344 delay times under dual-fuel engine conditions, *Fuel* 288 (2021) 119650.
- 345 [10] K. Hakimov, F. Arafin, K. Aljohani, K. Djebbi, E. Ninnemann, S. S.
346 Vasu, A. Farooq, Ignition delay time and speciation of dibutyl ether at
347 high pressures, *Combustion and Flame* 223 (2021) 98–109.

- 348 [11] M. Alabbad, Y. Li, K. AlJohani, G. Kenny, K. Hakimov, M. Al-lehaibi,
349 A.-H. Emwas, P. Meier, J. Badra, H. Curran, A. Farooq, Ignition delay
350 time measurements of diesel and gasoline blends, *Combustion and Flame*
351 222 (2020) 460–475.
- 352 [12] D. Glushkov, A. Kosintsev, G. Kuznetsov, V. Vysokomorny, Numeri-
353 cal simulation of ignition of a typical gel fuel particle, based on organic
354 polymer thickener, in a high-temperature air medium, *Acta Astronau-*
355 *tica* 178 (2021) 272–284.
- 356 [13] H. Wang, R. Xu, K. Wang, C. T. Bowman, R. K. Hanson, D. F. David-
357 son, K. Brezinsky, F. N. Egolfopoulos, A physics-based approach to mod-
358 eling real-fuel combustion chemistry - I. Evidence from experiments, and
359 thermodynamic, chemical kinetic and statistical considerations, *Com-*
360 *bustion and Flame* 193 (2018) 502–519.
- 361 [14] R. Xu, K. Wang, S. Banerjee, J. Shao, T. Parise, Y. Zhu, S. Wang,
362 A. Movaghar, D. J. Lee, R. Zhao, X. Han, Y. Gao, T. Lu, K. Brezin-
363 sky, F. N. Egolfopoulos, D. F. Davidson, R. K. Hanson, C. T. Bowman,
364 H. Wang, A physics-based approach to modeling real-fuel combustion
365 chemistry II. Reaction kinetic models of jet and rocket fuels, *Combus-*
366 *tion and Flame* 193 (2018) 520–537.
- 367 [15] K. D. Wan, C. Barnaud, L. Vervisch, P. Domingo, Chemistry reduction
368 using machine learning trained from non-premixed micro-mixing model-
369 ing: Application to DNS of a syngas turbulent oxy-flame with side-wall
370 effects, *Combustion and Flame* 220 (2020) 119–129.

- 371 [16] P. P. Popov, D. A. Buchta, M. J. Anderson, L. Massa, J. Capecelatro,
372 D. J. Bodony, J. B. Freund, Machine learning-assisted early ignition
373 prediction in a complex flow, *Combustion and Flame* 206 (2019) 451–
374 466.
- 375 [17] A. Chatzopoulos, S. Rigopoulos, A chemistry tabulation approach via
376 Rate-Controlled Constrained Equilibrium (RCCE) and Artificial Neu-
377 ral Networks (ANNs), with application to turbulent non-premixed
378 CH₄/H₂/N₂ flames, *Proceedings of the Combustion Institute* 34 (1)
379 (2013) 1465–1473.
- 380 [18] L. L. C. Franke, A. K. Chatzopoulos, S. Rigopoulos, Tabulation of com-
381 bustion chemistry via Artificial Neural Networks (ANNs): Methodology
382 and application to LES-PDF simulation of Sydney flame L, *Combustion
383 and Flame* 185 (2017) 245–260.
- 384 [19] K. D. Wan, S. Hartl, L. Vervisch, P. Domingo, R. Barlow, C. Hasse,
385 Combustion regime identification from machine learning trained by Ra-
386 man/Rayleigh line measurements, *Combustion and Flame* 219 (2020)
387 168–274.
- 388 [20] Z. Zhao, Z. Chen, S. Chen, Correlations for the ignition delay times of
389 hydrogen/air mixtures, *Chinese Science Bulletin* 56 (2) (2011) 215–221.
- 390 [21] Y. Snchez-Borroto, R. Piloto-Rodriguez, M. Errasti, R. Sierens, S. Ver-
391 helst, Prediction of Cetane Number and Ignition Delay of Biodiesel Us-
392 ing Artificial Neural Networks, *Energy Procedia* 57 (2014) 877–885.

- 393 [22] W. Liu, J. Zhang, Z. Huang, D. Han, Applicability of high dimen-
394 sional model representation correlations for ignition delay times of n-
395 heptane/air mixtures, *Frontiers in Energy* 13 (2) (2019) 367–376.
- 396 [23] A. Jach, M. Zbikowski, K. Malik, A. Teodorczyk, Ignition delay time
397 model based on a deep neural network, in: *Proceedings of the 27th*
398 *International Colloquium on the Dynamics of Explosions and Reactive*
399 *Systems*, Institute for Dynamics of Explosions and Reactive Systems,
400 Beijing, China, 2019, p. 65.
- 401 [24] Y. Cui, Q. Wang, H. Liu, Z. Zheng, H. Wang, Z. Yue, M. Yao, De-
402 velopment of the ignition delay prediction model of n-butane/hydrogen
403 mixtures based on artificial neural network, *Energy and AI* 2 (2020)
404 100033.
- 405 [25] H.-T. Nguyen, P. Domingo, L. Vervisch, P.-D. Nguyen, Machine learning
406 for integrating combustion chemistry in numerical simulations, *Energy*
407 and *AI* 5 (2021) 100082.
- 408 [26] T. Ding, T. Readshaw, S. Rigopoulos, W. Jones, Machine learning tabu-
409 lation of thermochemistry in turbulent combustion: An approach based
410 on hybrid flamelet/random data and multiple multilayer perceptrons,
411 *Combustion and Flame* 231 (2021) 111493.
- 412 [27] H. Liu, H.-q. Tian, Y.-f. Li, Comparison of two new ARIMA-ANN and
413 ARIMA-Kalman hybrid methods for wind speed prediction, *Applied*
414 *Energy* 98 (2012) 415–424.

- 415 [28] L. T. Le, H. Nguyen, J. Dou, J. Zhou, A Comparative Study of PSO-
416 ANN, GA-ANN, ICA-ANN, and ABC-ANN in Estimating the Heating
417 Load of Buildings Energy Efficiency for Smart City Planning, Applied
418 Sciences 9 (13) (2019) 2630.
- 419 [29] Y. Zhang, G. Pan, B. Chen, J. Han, Y. Zhao, C. Zhang, Short-term
420 wind speed prediction model based on GA-ANN improved by VMD,
421 Renewable Energy 156 (2020) 1373–1388.
- 422 [30] D. G. Goodwin, R. L. Speth, H. K. Moffat, B. W. Weber, Cantera: An
423 Object-oriented Software Toolkit for Chemical Kinetics, Thermodynam-
424 ics, and Transport Processes, <https://www.cantera.org>, version 2.4.0
425 (2018).
- 426 [31] M. Abadi, A. Agarwal, P. Barham, E. Brevdo, Z. Chen, C. Citro, G. S.
427 Corrado, A. Davis, J. Dean, M. Devin, S. Ghemawat, I. Goodfellow,
428 A. Harp, G. Irving, M. Isard, Y. Jia, R. Jozefowicz, L. Kaiser, M. Kud-
429 lur, J. Levenberg, D. Mané, R. Monga, S. Moore, D. Murray, C. Olah,
430 M. Schuster, J. Shlens, B. Steiner, I. Sutskever, K. Talwar, P. Tucker,
431 V. Vanhoucke, V. Vasudevan, F. Viégas, O. Vinyals, P. Warden, M. Wat-
432 tenberg, M. Wicke, Y. Yu, X. Zheng, TensorFlow: Large-Scale Ma-
433 chine Learning on Heterogeneous Systems, software available from ten-
434 sorflow.org (2015).
435 URL <http://tensorflow.org/>
- 436 [32] D. P. Kingma, J. Ba, Adam: A Method for Stochastic Optimization,
437 arXiv:1412.6980 [cs].

- 438 [33] Y. Zhu, S. Li, D. F. Davidson, R. K. Hanson, Ignition delay times of
439 conventional and alternative fuels behind reflected shock waves, Pro-
440 ceedings of the Combustion Institute 35 (1) (2015) 241–248.
- 441 [34] A. R. De Toni, M. Werler, R. M. Hartmann, L. R. Cancino, R. Schiel,
442 M. Fikri, C. Schulz, A. A. M. Oliveira, E. J. Oliveira, M. I. Rocha, Igni-
443 tion delay times of Jet A-1 fuel: Measurements in a high-pressure shock
444 tube and a rapid compression machine, Proceedings of the Combustion
445 Institute 36 (3) (2017) 3695–3703.
- 446 [35] E. Hu, L. Pan, Z. Gao, X. Lu, X. Meng, Z. Huang, Shock tube study
447 on ignition delay of hydrogen and evaluation of various kinetic models,
448 International Journal of Hydrogen Energy 41 (30) (2016) 13261–13280.
- 449 [36] S. Lee, S. Song, Hydrogen effects on ignition delay time of methyl bu-
450 tanoate in a rapid compression machine, International Journal of Energy
451 Research 45 (4) (2021) 5602–5618.
- 452 [37] S. Frolov, S. Medvedev, V. Basevich, F. Frolov, Self-ignition of hydro-
453 carbonhydrogenair mixtures, International Journal of Hydrogen Energy
454 38 (10) (2013) 4177–4184.